Coherent and dissipative dc transport in quasi-one-dimensional systems of coupled polyaniline chains

R. Hey, F. Gagel, and M. Schreiber
Institut für Physik, Technische Universität Chemnitz-Zwickau, D-09107 Chemnitz, Federal Republic of Germany

K. Maschke
Institut de Physique Appliquée, Ecole Polytechnique Fédérale, CH 1015 Lausanne, Switzerland
(Received 22 July 1996; revised manuscript received 24 September 1996)

We present numerical studies on the conductance of coupled polyaniline chains. Our investigation is based on a tight-binding Hamiltonian, which comprises the description of the single polymer chains as well as interchain interactions. Phase-breaking processes are included in the Hamiltonian via imaginary self-energy corrections within the Green's-function formalism describing the system. The variation of these self-energies allows one to describe the transport over the full range in between the coherent and dissipative regimes. In the coherent limit we observe a transition from exponential to power-law localization upon increasing the size of the cross section of the quasi-one-dimensional systems. This behavior is all the more pronounced, the smaller the disorder in the specimen is. Upon introducing dissipation into the system we can identify metallic, insulating, and critical samples of polyaniline. These observations are consistent with recent experimental results, which characterize polyaniline-camphor sulfonic acid as a system at the metal-insulator transition. [S0163-1829(97)07307-4]

I. INTRODUCTION

It is well known that protonation of the emeraldine form of polyaniline (PANI) raises the conductivity of the polymer up to 10 orders of magnitude and leads to a phase segregation into conducting and insulating domains. Whereas in some PANI-Cl samples these domains seem to consist of single polymer chains,[1] recent experiments[2] suggest the existence of three-dimensional (3D) conducting islands consisting of coupled protonated emeraldine chains for polyaniline-camphor sulfonic acid (PANI-CSA). In the former case, the sudden turning on of the Curie component of the paramagnetic susceptibility at $T=50$ K indicates low-temperature polaron localization on the chain. At even lower temperatures, two polarons may combine, forming spinless bipolarons, if they are in sufficient proximity,[3] leading to a change of the behavior of the temperature-dependent susceptibility below $T=10$ K.[4] Both processes are consequences of Peierls distortions, the first one being induced by changes in the spin density, the second one being caused by rearrangement of π bonds.

In this paper, we focus on the transport properties of crystalline PANI. In contrast to 1D PANI, crystalline samples exhibit significant interactions between the individual chains that stabilize the polymer against Peierls transitions[4] and furthermore prevent the electrons from 1D localization due to disorder effects. Because of the alignment of the ordered polymer chains in oriented samples, crystalline PANI is a typical example for a highly anisotropic (quasi-1D) disordered system. We calculate the conductance of crystalline PANI samples in the coherent limit as well as under the influence of dissipative processes, thus providing two tools for the characterization of electronic transport in the polymer.

There is an ongoing debate about whether a bipolaron lattice or a polaronic structure is linked to the metallic regime in PANI.[5,6] A few years ago, some theoretical works[7–9] were published that focus on the transport properties of protonated emeraldine in the 1D bipolaron model. In this approach, bipolarons are considered as random dimer defects in an otherwise ordered lattice. Such defects lead to resonances of perfect transmission in the energy spectrum, indicating the existence of isolated metallic states within a finite-sized sample. Recent investigations have shown that the internal symmetry of such defects is not even a necessary condition[10] for the occurrence of such transmission peaks.

The constriction concerning the size of the sample is very important and often leads to confusion in the literature. As pointed out in Refs. 11 and 12, the transmission spectrum of random dimer models exhibits so-called cluster-core regions. For energies outside these regions, resonance states decay exponentially as in a purely random chain and therefore can be referred to as Azbel resonances.[13] Inside a cluster core, resonance states decay only algebraically, and if the Fermi energy falls within this region, the conductance is significantly large. But as such a cluster region gets narrower and narrower when the length of the chain is increased, random dimer chains do not exhibit a metal-insulator transition in the infinite length limit. Therefore we doubt that such a model can explain the high conductivities achieved in large crystalline polymer samples.

More detailed investigations on the conduction mechanism of the bipolaronic structure have shown that a band gap opens at the Fermi energy in the ordered system.[14] However, if the bipolarons are randomly distributed along the polymer chain, the density of states is produced at the Fermi level by band broadening. Thus, the authors of Ref. 14 conclude that disorder effects play an essential role in the conduction mechanism of PANI, leading to a high conductivity. This assumption certainly has its validity with respect to small 1D

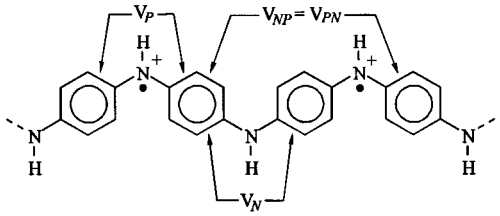

FIG. 1. Protonated emeraldine in the polaron-lattice structure. V_N, V_P, V_{PN}, and V_{NP} indicate transfer elements in the 1D TB model.

structures as in dilute systems[15] or substituted PANI derivatives,[6] where interchain diffusion is suppressed. However, as mentioned above its application to quasi-1D PANI samples is highly doubtful.[16]

Crystalline regions of PANI are formed by arrays of weakly coupled polymer chains. As pointed out in Refs. 17 and 18, there is strong experimental evidence for a highly stable ordered polaron lattice (see Fig. 1) in such regions. Thus it is generally assumed that the ordered polaron form of PANI is responsible for the high conductance of quasi-1D protonated emeraldine,[19] and we restrict ourselves to the investigation of the transport properties of coupled systems composed of this PANI structure. The effect of various kinds of defects on the conductance of isolated 1D PANI chains will be discussed in a forthcoming paper.

The electronic structures of different forms of PANI chains have been widely studied.[19,20] As described in detail in Ref. 21, we use these results to derive the parameters needed for the description of the polymer chains within a tight-binding (TB) model. In this picture, the polymer backbone with its rings and nitrogen bridges is simplified as a linear chain of fictitious orbitals corresponding to the rings. Each orbital can be characterized by its TB parameters, that is to say its site energy and its transfer matrix elements to neighboring sites. These transfer energies differ for different nitrogen bridges. In this way a polymer chain can be represented by a respective TB matrix, which contains the parameters of the single orbitals that build up the chain. Using suitable TB parameters, the band structure of the single polymer strands in the vicinity of the Fermi energy can be reproduced.[21]

We point out that our model Hamiltonian should be distinguished from local bond-length descriptions as introduced in Refs. 8, 10, and 22, which are suitable for small 1D (oligomer) systems. In this paper we use a more coarse model, which enables us to calculate the transport properties of relatively large samples of coupled polymer chains. Nevertheless, the TB parameters we use to describe the single polymer chains are based on band-structure calculations, which take geometrical details on the bond-length scale explicitly into account.[20]

TABLE I. TB parameters of the single PANI chains and of the semi-infinite leads connecting the respective sample to the current-driving electron reservoirs.

	TB parameter	[eV]
Site energies	E_B	-7.64
	E_0	-7.5
Nearest-neighbor transfer elements	V_N	$+0.73$
	V_P	$+0.7$
	V	$+1.0$
Next-nearest-neighbor transfer element	$V_{PN}=V_{NP}$	-0.07

In addition to the 1D TB model, interchain transfer elements are introduced, which couple the lattice sites of the single chains weakly to nearest-neighbor sites on adjacent chains. On the basis of this approach we derive the scattering coefficients of the coupled-chain system using a Green's-function method, which are then used to calculate the dc conductance within the multichannel Landauer-Büttiker approach.[23] A similar approach has been made by Stafström[24] for doped polyacetylene on the basis of the transfer-matrix method in the limit of coherent transport.

As described by D'Amato and Pastawski,[25] dissipative processes can be included by an imaginary self-energy correction in the Green's function of the system. As the variation of this parameter allows us to describe the transport for arbitrary dissipation, it can be identified with a nonlinear temperature scale. We use this approach to study the effects of finite temperature on the transport properties of the system.

II. THE MODEL

As depicted in Fig. 2, we consider a system of coupled protonated emeraldine chains. In this example, we have $MN=25$ transport channels and LMN lattice sites in the system. The individual chains are described by respective 1D TB lattices. According to Ref. 21, we choose the TB parameters as listed in Table I. E_B is the site energy of the (benzenoid) lattice sites, the transfer elements V_N and V_P between nearest-neighbor sites as well as V_{NP} and V_{PN} between next-nearest-neighbor sites in the chain are illustrated in Fig. 1.[26]

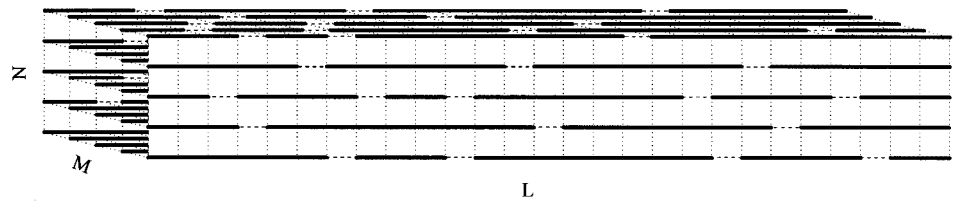

FIG. 2. PANI in the model of coupled polymer chains. The thick lines represent the single PANI chains. Between these chains, weak interactions exist, represented by the transfer elements V_{EE} (end-to-end coupling, broken lines) and $V_\perp$ (lateral coupling, dotted lines).

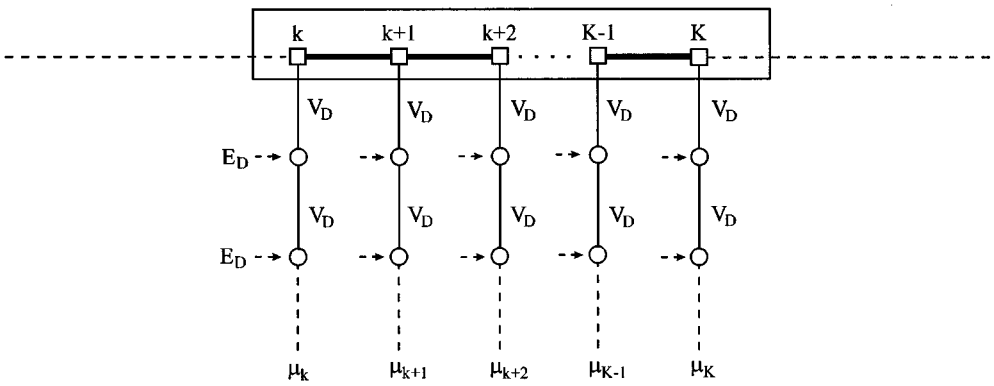

FIG. 3. Model of a single PANI chain. The 1D array (indicated by the rectangular box) of sites (depicted as squares) corresponds to a thick line in Fig. 2, beginning at an arbitrary lattice site k and consisting of $K-k+1$ lattice sites in the case shown here. The broken lines on either side of the chain represent either end-to-end couplings or couplings of the chain to semi-infinite leads at the faces of the system. In order to introduce dissipation, the lattice sites are connected to electron reservoirs via additional side channels (which are not shown in Fig. 2 for convenience).

Interchain coupling is accounted for by introducing transfer elements $V_\perp$ between nearest-neighbor sites on adjacent chains in other transport channels (lateral interchain coupling). As the cross section of the considered system is chosen to be a square lattice (see Fig. 2), each lattice site in the system is connected either to 2, 3, or 4 sites in the neighboring transport channels, depending on its position in the system. Furthermore, sites located at the ends of a chain are additionally coupled to the nearest-neighbor sites of the adjacent chain in the same transport channel (end-to-end coupling V_{EE}).

In the present study, we use the Landauer-Büttiker theory[23] to calculate the conductance of the coupled PANI chain systems. As usual in this approach, we connect the sample on either side to a respective electron reservoir via perfectly conducting semi-infinite leads (not shown in Fig. 2 for convenience). The chemical potentials of the electron reservoirs are chosen to be μ_{L} (μ_{R}) on the left-hand side (right-hand side) of the system, respectively. The condition $\mu_{\mathrm{L}}>\mu_{\mathrm{R}}$ defines a voltage drop from the left-hand side to the right-hand side, giving rise to a net electronic current through the system.

Dissipative processes can be introduced by connecting the lattice sites to respective additional electron reservoirs via side channels (see Fig. 3).[25] As these reservoirs only serve to randomize the phase of the electrons, the net current into the side channels must be zero. Thus for each electron leaving the system via such a side channel another one is scattered back into the sample. As the phases of the electrons entering and leaving the system are not correlated, such an event corresponds to a dissipative scattering process.

The scattering probabilities needed to evaluate the currents in the single channels (and thus the conductance of the system) are calculated within the framework of a Green's-function method[27] as follows. Neglecting the transfer elements in the polymer system, the influence of the semi-infinite leads connecting the sample to the bias-defining electron reservoirs on the site energies at the faces of the quasi-1D system can be accounted for by the self-energy function[25]

$$\Sigma=\frac{E-E_0}{2}-i\left[V^2-\left(\frac{E-E_0}{2}\right)^2\right]^{1/2}, \tag{1}$$

where E_0 denotes the site energy and V the transfer element in the leads. Here E is the energy of the incoming electron.

A side channel at a lattice site n gives rise to a self-energy function Σ_{D} comprising the influence of dissipation. Σ_{D} is of the same type as Σ; the parameters E_0 and V in Eq. (1) merely have to be replaced by the site energy $E_{\mathrm{D}}(n)$ and the transfer element $V_{\mathrm{D}}(n)$ in the side chain at lattice site n, respectively. For convenience, we restrict ourselves to constant values of E_{D} and V_{D} along the system throughout this paper: $E_{\mathrm{D}}(n)\equiv E_{\mathrm{D}}$ and $V_{\mathrm{D}}(n)\equiv V_{\mathrm{D}}$. Choosing E_{D} to be equal to the energy E of the incoming electron, one obtains a purely imaginary damping $-iV_{\mathrm{D}}$ as a self-energy correction to the respective site energy[25] and the parameter V_{D} controls the strength of inelastic scattering. Thus the approach used here is fully equivalent with the introduction of a finite lifetime of electrons in a given state as discussed by McLennan, Lee, and Datta.[27] (In Ref. 27, the authors used the Kadanoff-Baym formalism[28] in order to derive exactly this parameter V_{D} as a function of temperature within a many-particle approach.) Consequently, the matrix elements of the Green's function G_0 at the (isolated) lattice sites at the faces of the system where one obtains self-energy corrections due to lateral chains and semiinfinite leads read

$$G_0(n,m)=\frac{\delta_{nm}}{E-E_{\mathrm{B}}+iV_{\mathrm{D}}-(E-E_0)/2+i\sqrt{V^2-(E-E_0)^2/4}}, \tag{2}$$

and in the bulk of the system where one obtains solely contributions due to the lateral chains they read

$$G_0(n,m)=\frac{\delta_{nm}}{E-E_{\mathrm{B}}+iV_{\mathrm{D}}}. \tag{3}$$

Due to the neglect of the transfer elements between the sites n and m of the system, the matrix $\underline{G}_0$ is diagonal. These transfer elements can be introduced[27] via the Dyson equation

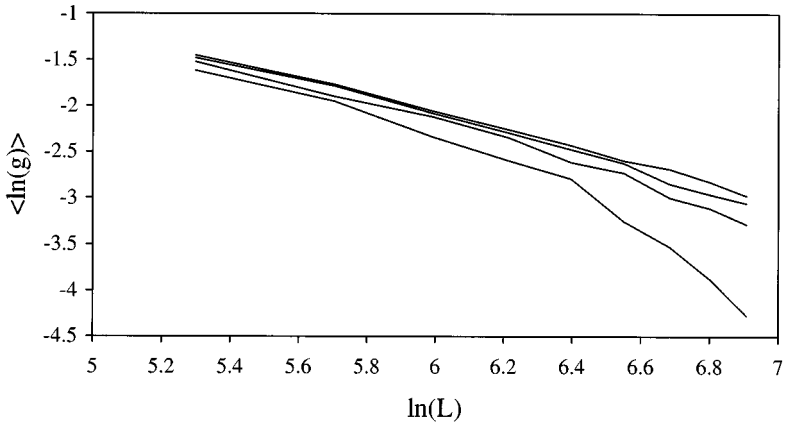

FIG. 4. $\langle \ln g \rangle$ as a function of $\ln L$ for systems of the extension $3\times3\times L$, $4\times4\times L$, $5\times5\times L$, and $6\times6\times L$ (from bottom to top) and an average length $\langle l \rangle = 100$ of the single chains, $V_{\mathrm{EE}}, V_{\perp} \in [0\ \mathrm{eV}, 0.08\ \mathrm{eV}]$.

$(\underline{1} - \underline{G}_0 \underline{V})\underline{G}^{\mathrm{R}} = \underline{G}_0$, where $\underline{V}$ denotes the matrix of the transfer elements. The retarded Green's function matrix $\underline{G}^{\mathrm{R}}$ contains the probability amplitudes for the propagation of an electron between the LMN sites of the system. The transmission probabilities in the single channels can be derived by multiplying the respective squared absolute values of $\underline{G}^{\mathrm{R}}$ with the group velocities of the corresponding side channels and semi-infinite leads.[29] If we number the side channels like the lattice sites with $k,k' = 1,\ldots,LMN$ and the transport channels on the left-hand side (right-hand side) by $i = 1,\ldots,MN$ ($j = LMN - MN + 1,\ldots,LMN$), these transmission probabilities read

$$p_{ji} = |G^{\mathrm{R}}(j,i)|^2 4V^2 \sin^2(qa), \tag{4}$$

$$p^{\mathrm{D}}_{jk} = |G^{\mathrm{R}}(j,k)|^2 4V \sin(qa) V_{\mathrm{D}}, \tag{5}$$

$$p^{\mathrm{D}}_{k'k} = |G^{\mathrm{R}}(k',k)|^2 4V^2_{\mathrm{D}}. \tag{6}$$

Choosing the same index number for the side channels and the semi-infinite leads at the faces of the system simplifies the notation. Transmission probabilities involving dissipative side channels are distinguished by the superscript D.

The dimensionless conductance (normalized to the number of transport channels) of the coupled polymer system is then given by

$$g = \frac{1}{MN}\left(\sum_i \sum_j p_{ji} + \sum_k \chi_k \sum_j p^{\mathrm{D}}_{jk} \right). \tag{7}$$

The chemical potentials χ_k at the lattice sites k are obtained from the current conservation condition:[30]

$$0 = \frac{h}{2e} I_k = \sum_i p^{\mathrm{D}}_{ki}(\mu_k - \mu_{\mathrm{L}}) + \sum_j p^{\mathrm{D}}_{kj}(\mu_k - \mu_{\mathrm{R}}) + \sum_{k'} p^{\mathrm{D}}_{kk'}(\mu_k - \mu_{k'}), \quad k = 1,\ldots,LMN. \tag{8}$$

Using $\mu_k = \mu_{\mathrm{R}} + \chi_k(\mu_{\mathrm{L}} - \mu_{\mathrm{R}})$ and $\mu_{\mathrm{L}} - \mu_{\mathrm{R}} \neq 0$, Eq. (8) can be written in the form

$$\sum_i p^{\mathrm{D}}_{ki} = \chi_k \left(\sum_i p^{\mathrm{D}}_{ki} + \sum_j p^{\mathrm{D}}_{kj} + \sum_{k'} p^{\mathrm{D}}_{kk'} \right) - \sum_{k'} \chi_{k'} p^{\mathrm{D}}_{kk'}, \quad k = 1,\ldots,LMN. \tag{9}$$

Thus we obtain a linear system of equations for the determination of the χ_k.

To summarize the numerical solution procedure, we proceed as follows. First we set up the $\underline{G}_0$ matrix [Eqs. (2) and (3)] and introduce transfer interactions between neighboring lattice sites via the Dyson equation. We thus obtain the scattering probabilities (4)–(6), which can be used to determine the chemical potentials χ_k at the single lattice sites of the system by solving the respective inhomogeneous linear system of Eq. (9). The conductance g is fully determined by the chemical potentials and the transmission probabilities of the system [see Eq. (7)].

III. NUMERICAL RESULTS

A. Coherent limit

In this section we present numerical results for the conductance of coupled PANI chain systems. Figure 4 shows g as a function of the system length L. The configurational average $\langle \ln g \rangle$ is taken over 100 systems. (Because of its self-averaging properties, we use $\langle \ln g \rangle$ and not $\ln\langle g \rangle$.[31]) As in this example the position of the end-to-end couplings is randomly distributed (subject to the restriction that the minimum chain length allowed is 10 lattice sites) and the transfer elements V_{EE} and $V_{\perp}$ between the single chains are taken from a uniform distribution, these ensembles comprise two types of disorder, which we will refer to as chain-length disorder and interchain disorder, respectively.

One can clearly observe that systems with a cross section of 3×3 sites essentially show 1D behavior. This behavior becomes more and more pronounced as the length of the system is increased. On the contrary, an increase of the cross section suppresses this behavior and one obtains a nearly linear dependence of $\langle \ln g \rangle$ on $\ln L$. We thus conclude that there is a transition from exponential to power-law localization upon increasing the cross section of quasi-1D PANI systems. Such a power-law dependence was proposed by Last and Thouless[32] to describe a region of intermediate behavior between metallic and localized states.

This feature becomes even more pronounced upon restriction to chain-length disorder. Figure 5 shows data for the same ensemble of systems as in Fig. 4; all the transfer elements between the single chains are now equal. This choice corresponds to highly ordered, crystalline PANI samples. Additionally, data for the ensemble with the largest cross

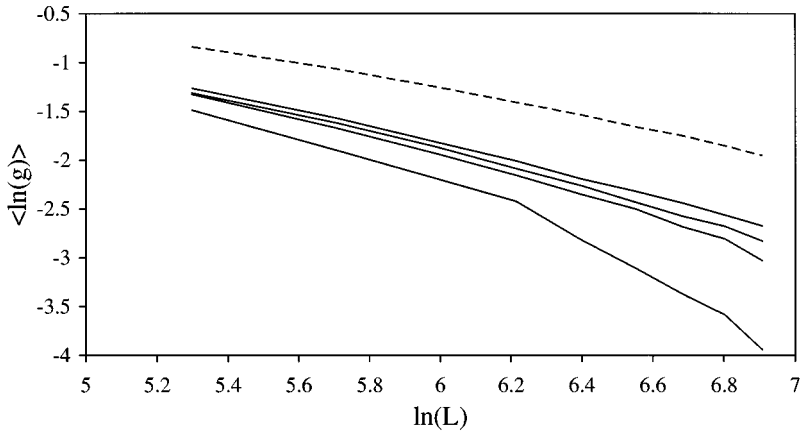

FIG. 5. $\langle \ln g \rangle$ as a function of $\ln L$ for the same ensemble of systems as in Fig. 4, but with constant interchain interactions: $V_{EE}=V_{\perp}=0.04$ eV (full lines). The broken line shows the case $6\times6\times L$ with $\langle l \rangle = 200$.

section and a longer average chain length are included. Figure 5 shows in comparison with Fig. 4 that the power-law dependence of $\langle \ln g \rangle$ on $\ln L$ is the more pronounced the smaller the amount of disorder and the greater the average length of the single chains. Consequently the power-law exponent α, determined from these conductance data ($\langle \ln g \rangle = \ln L^{-\alpha} + \text{const}$) is largest in the case of combined chain-length disorder and interchain disorder ($\alpha \approx 0.93$) and smaller in the case of restriction to chain-length disorder: $\alpha \approx 0.85$ (0.64) for an average single-chain length of 100 (200) lattice sites.

We wish to point out that for a fixed cross section the system should always exhibit exponential localization in the case of $L \to \infty$. In quasi-1D systems it is the competition between the size of the cross section and the system length L that determines the character of localization. Thus the power-law dependence can only be observed if the system length is sufficiently small in comparison to the cross section. Such systems can be related to (experimentally accessible) samples of coupled PANI chains of finite spatial extension.

The results presented in this section are clearly in contrast to the results for polyacetylene obtained by Stafström[24,33] on the basis of an approach very similar to the one used in this work. For certain polyacetylene samples, his numerical calculations yielded an increase of the conductance with the system length in the regime of $L \leqslant 1000$ lattice sites. In our model we cannot expect such behavior, because the transmission probability of the (perfectly ordered) single PANI chains is almost 1 (see Ref. 21) (small deviations from this value are due to contact resistances) so that the disorder introduced by the coupling of the single chains to a quasi-1D system can only reduce the transmission probability and consequently the conductance decays with increasing system size.

B. Effects of finite temperature

In this section, we focus on the dependence of the transport properties of quasi-1D PANI samples on dissipative processes. Experiments by Reghu *et al.*[34] concerning the temperature dependence of the resistivity characterize PANI-CSA as a system at the metal-insulator transition. Using the logarithmic derivative of the conductivity σ, the authors define an activation energy

$$W(T) = \frac{\Delta \ln \sigma(T)}{\Delta \ln T}, \tag{10}$$

which can be used to identify metallic, insulating, and critical samples of PANI-CSA. Insulating d-dimensional systems obey Mott's law $\sigma(T) \propto \exp[-(T_0/T)^{\gamma}]$ with $\gamma = 1/(1+d)$, which leads to an activation energy

$$W_I(T) = \frac{1}{\gamma}\left(\frac{T_0}{T}\right)^{\gamma}. \tag{11}$$

Consequently, such insulating systems are characterized by a straight line with slope $-\gamma$ in a $\ln W - \ln T$ diagram.[34] According to Larkin and Khmel'nitskii,[35] the resistivity of critical systems follows a power-law behavior $\rho(T) \propto T^{-\beta}$, which leads to a temperature-independent activation energy

$$W_C = \beta. \tag{12}$$

Metallic samples exhibit a linear dependence of $\ln W$ on $\ln T$ with positive slope.[34]

In the framework of this paper, we cannot draw any conclusions about the exponents because we use a nonlinear temperature scale rather then an explicit temperature dependence. (The introduction of such an explicit temperature scale is computationally too expensive in the case of quasi-1D systems. In a forthcoming paper we will use an approach suggested by McLennan, Lee, and Datta[27] in order to introduce an explicit temperature dependence of the conductance for 1D PANI.) Therefore we cannot expect a linear dependence of $\ln W$ as a function of $\ln T$. Instead we focus on the dependence of the conductance on V_D to distinguish qualitatively between metallic, insulating, and critical behavior.

Figure 6 shows the dependence of the conductance on the inelastic scattering strength. The upper curve in Fig. 6 shows a metallic specimen, because the conductance is strongly decaying with growing V_D. The lower curve characterizes a sample in the insulating regime, where the conductivity increases with the dissipation strength for small V_D. The curve in the middle depicts a (with respect to the V_D scale) critical system, as can be seen from the linear dependence of $\ln g$ on $\ln V_D$. Thus our results show that the transport behavior of coupled PANI chain systems is extremely sensitive to the specific sample configuration. Using the same average length of the individual chains and the same (average) value for the

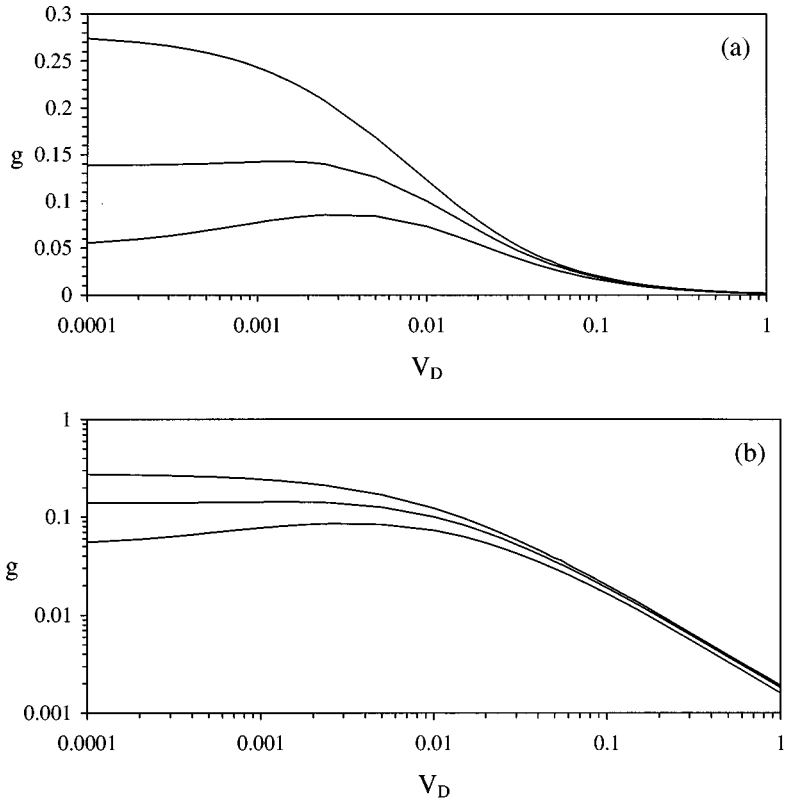

FIG. 6. $g(V_D)$ for three PANI samples of extension $3\times3\times L$, $\langle l\rangle=100$ and $V_{EE}=V_{\perp}=0.04$ eV using (a) a logarithmic and (b) a double-logarithmic scale.

interchain transfer elements, we obtain sample realizations with qualitatively different transport behavior. Whether such a sample is metallic, critical, or insulating is determined by the electronic interference pattern, which constitutes a fingerprint of the microscopic details of the specimen.

IV. CONCLUSIONS

In this paper, we have presented numerical studies on the conductance of quasi-1D PANI systems. We have used two methods to investigate the nature of electron localization in these systems. On the one hand, by averaging $\ln g$ over an ensemble of 100 samples we observe a transition from exponential to power-law localization upon increasing the system's cross section relative to the system length in the coherent limit. This behavior can be interpreted as an indication for the existence of a critical region between insulating and metallic states. On the other hand, the dependence of the conductance on the strength of dissipation displays metallic, critical, and insulating behavior for specific sample realizations, respectively. Thus in accordance with recent experiments[36] our numerical studies indicate that doped PANI can form systems at the metal-insulator phase boundary.

[1] K. Mizoguchi, M. Nechtschein, J.-P. Travers, and C. Menardo, Phys. Rev. Lett. **63**, 66 (1989).
[2] Z. H. Wang, C. Li, E. M. Scherr, A. G. MacDiarmid, and A. J. Epstein, Phys. Rev. Lett. **66**, 1745 (1991).
[3] A. J. Epstein, J. M. Ginder, F. Zuo, H.-S. Woo, D. B. Tanner, A. F. Richter, M. Angelopoulos, W.-S. Huang, and A. G. Mac Diarmid, Synth. Met. **21**, 63 (1987).
[4] N. S. Sariciftci, A. J. Heeger, and Y. Cao, Phys. Rev. B **49**, 5988 (1994).
[5] P. K. Kahol, N. J. Pinto, E. J. Berndtsson, and B. J. McCormick, J. Phys. Condens. Matter **6**, 5631 (1994).
[6] P. K. Kahol, V. Pendse, N. J. Pinto, M. Traore, W. T. K. Stevenson, B. J. McCormick, and J. N. Gundersen, Phys. Rev. B **50**, 2809 (1994).
[7] H.-L. Wu and P. Phillips, Phys. Rev. Lett. **66**, 1366 (1991).
[8] H. Dücker, M. Struck, Th. Koslowski, and W. von Niessen, Phys. Rev. B **46**, 13 078 (1992).
[9] D. S. Galvão, D. A. dos Santos, B. Laks, C. P. de Melo, and M. J. Caldas, Phys. Rev. Lett. **63**, 786 (1989).
[10] F. C. Lavarda, M. C. dos Santos, D. S. Galvão, and B. Laks, Phys. Rev. Lett. **73**, 1267 (1994).
[11] A. K. Sen and S. Gangopadhyay, Physica A **186**, 270 (1992).
[12] S. Gangopadhyay and A. K. Sen, J. Phys. Condens. Matter **4**, 9939 (1992).
[13] M. Ya. Azbel, Phys. Rev. B **28**, 4106 (1983).
[14] P. A. Schulz, D. S. Galvão, and M. J. Caldas, Phys. Rev. B **44**, 6073 (1991).
[15] C. Fite, Y. Cao, and A. J. Heeger, Solid State Commun. **73**, 607 (1990).
[16] J. L. Brédas, A. J. Epstein, and A. G. MacDiarmid, Phys. Rev. Lett. **65**, 526 (1990).
[17] S. M. Yang and C. P. Li, Synth. Met. **55-57**, 636 (1993).
[18] J. M. Ginder, A. F. Richter, A. G. MacDiarmid, and A. J. Epstein,

Solid State Commun. **63**, 97 (1987).
[19] S. Stafström, J. L. Brédas, A. J. Epstein, H. S. Woo, D. B. Tanner, W. S. Huang, and A. G. MacDiarmid, Phys. Rev. Lett. **59**, 1464 (1987).
[20] D. S. Boudreaux, R. R. Chance, J. F. Wolf, L. W. Shacklette, J. L. Brédas, B. Thémans, J. M. André, and R. Silbey, J. Chem. Phys. **85**, 4584 (1986).
[21] R. Hey and M. Schreiber, J. Chem. Phys. **103**, 10 726 (1995).
[22] M. C. dos Santos and J. L. Brédas, Phys. Rev. Lett. **62**, 2499 (1989).
[23] M. Büttiker, Y. Imry, R. Landauer, and S. Pinhas, Phys. Rev. B **31**, 6207 (1985).
[24] S. Stafström, Synth. Met. **65**, 185 (1994).
[25] J. L. D'Amato and H. M. Pastawski, Phys. Rev. B **41**, 7411 (1990).
[26] The indices of the transfer elements refer to the types of nitrogen bridges linking the benzenoid rings. The index ''N'' indicates a neutral nitrogen bridge, the index ''P'' a polaronic one. As transport between nearest-neighbor (next-nearest-neighbor) sites involves 1 (2) nitrogen bridges, the respective transfer elements carry 1 (2) indices.
[27] M. J. McLennan, Y. Lee, and S. Datta, Phys. Rev. B **43**, 13 846 (1991).
[28] L. P. Kadanoff and G. Baym, *Quantum Statistical Mechanics* (Benjamin, New York, 1962).
[29] D. S. Fisher and P. A. Lee, Phys. Rev. B **23**, 6851 (1981).
[30] M. Schreiber and K. Maschke, Phys. Rev. B **44**, 3835 (1991).
[31] J. Sak and B. Kramer, Phys. Rev. B **24**, 1761 (1981).
[32] B. J. Last and D. J. Thouless, J. Phys. C **7**, 699 (1974).
[33] S. Stafström, Phys. Rev. B **51**, 4137 (1995).
[34] M. Reghu, C. O. Yoon, C. Y. Yang, D. Moses, P. Smith, A. J. Heeger, and Y. Cao, Phys. Rev. B **50**, 13 931 (1994).
[35] A. I. Larkin and D. E. Khmel'nitskii, Zh. Eksp. Teor. Fiz. **83**, 1140 (1982) [Sov. Phys. JETP **56**, 647 (1982)]
[36] M. Reghu, C. O. Yoon, D. Moses, A. J. Heeger, and Y. Cao, Phys. Rev. B **48**, 17 685 (1993).